CORE
Metadata, citation and similar papers at core.ac.uk
Provided by Advanced Electromagnetics (E-Journal)

ADVANCED ELECTROMAGNETICS, Vol. 3, No. 1, April 2014

A Novel Microwave Coaxial Slot Antenna for Liver Tumor Ablation

Hulusi Açıkgöz*, İbrahim Türer

*KTO Karatay University, Konya, Turkey
*corresponding author, E-mail: hulusi.acikgoz@karatay.edu.tr

Abstract

This paper is on the effect of a T-ring shape structure to enhance the capability of a microwave coaxial slot antenna (MCA) in the treatment of liver cancer. The MCA is composed of an interstitial coaxial line that is enclosed in a catheter. The T-ring shape structure is wrapped on the outer conductor of the MCA. Thanks to the new structure, the backward heating problem appearing in many coaxial antennas is reduced and the generated heat in front of the slot is higher than those for a classical MCA.

1. Introduction

According to [1], the number of liver cancers diagnosed throughout the world is increasing at an alarming rate. Also this rate is estimated to increase over the next few decades.
Liver cancers are two types: *Hepatocellular Carcinoma* (HCC) also called the primary liver cancer is the leading cause of liver tumor. In 2013, about 23,000 men and 8,000 women in the United States will be diagnosed with primary liver cancer. Most will be over 64 years old [2].
In some countries most malignant cancers are *metastatic*. In this case, the tumor begins at other parts of the body (colon, lungs, breasts, etc.) and *metastasize* (spread) to the liver [2].

Traditionally the most common option for treatment of liver cancer is the surgical resection of the tumor from the liver. This operation yields to 5 year survival rate of approximately 35%. For an untreated disease this rate is 0%. Unfortunately, only 10-20% of patients are eligible for liver resection. The main reasons are: the spread of the tumor to other parts of the liver, unfavorable tumor location, tumor size and high risk due to the associated cirrhosis or disease. In the case of patients with cirrhosis, the postoperative complications rate is about 42% [3].
The main alternatives to surgical resection are the ablation procedures that have the aim to kill the entire tumor without damaging the surrounding healthy tissue. These are divided into three categories: chemical, cold based and heat based ablations. In the case of the *chemical ablation* technique, ethanol is injected with small needle. This technique seems to give better results for small size tumors, less than 2 cm [4]. During the *cyrotherapy ablation* the intracellular and extracellular frizzing in tissue induce tumor cell death. The probes are cooled using liquid nitrogen. This technique is well suited for the treatment of large or multiple lesions. The freezing is monitored using intra-operative ultrasound. Currently, the most commonly used ablation procedure is *radio-frequency ablation* (RFA). The procedure requires the insertion of probes in the cancerous tissue and applying high frequency (~500 kHz) alternating current that causes frictional heat in a small area (1-2 mm) near the probes [5]. Although this technique allows tissue coagulation near the probe tip with low rate of bleeding and percutaneous application via relatively small probe, *microwave ablation* (MWA) becomes a promising technique that has several advantages to RFA. MWA uses a thin interstitial microwave antenna to heat tissue by applying electromagnetic radiation at microwave frequencies, usually 2.45 GHz. The main advantage of MWA is to perform faster heating and consequently the treatment of the cancer is shorter. Also, using MWA, larger lesions may be obtained by means of blood perfusion.

Most of studies are based on the use of microwave coaxial antenna (MCA) and focused on SAR distribution and heating effect caused in the vicinity of the antenna [6, 7, 8, 9,10]. These antennas are minimally invasive and capable to achieve more localized power deposition on the cancerous region of the liver. Different type of MCA has been studied in the literature. The most important are: dipole, slot and monopole antennas [7]. In this paper, we focus on the slotted MCA and particularly to its improvement to achieve better Specific Absorption Rate (SAR) pattern and to suppress the backward heating effect that is the common drawback of this type of antennas. This effect is represented in many SAR pattern as a “tail” along the coaxial feed line [11].

This paper presents a novel approach in the coaxial antenna design. In order to eliminated the backward heating effect along the antenna a T-ring shape structure is mounted on the outer conductor of the MCA.
In the second part of this paper, the single slot MCA and the proposed new MCA are presented. We also detail the electromagnetic and thermal analysis of the numerical models. Finally, numerical results on SAR and temperature distribution in the liver tissue which demonstrate that the new design of coaxial slot antenna seems to address the problem cited above and to achieve a highly localized SAR pattern.

2. Materials and method

2.1. The Single Slot MCA

The single slot microwave coaxial antenna used in this study is depicted in Figure 1. It is composed of inner and outer conductors, a dielectric between them and a catheter that is made of polytetrafluorethylene (PTFE). The catheter allows physical protection of the antenna and improves the electromagnetic coupling between the antenna and the liver tissue [7].

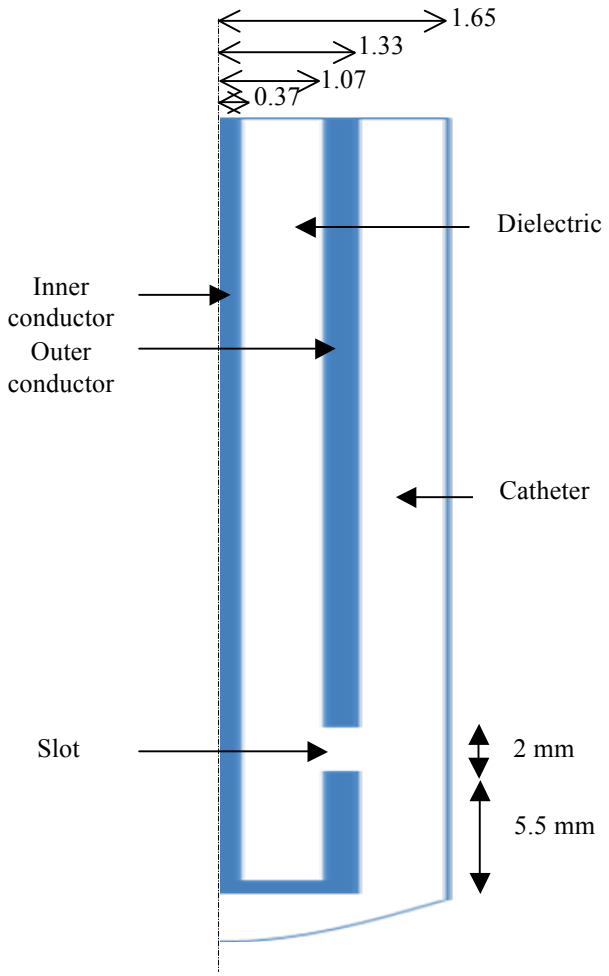

Figure 1: 2D Axisymetric view of the single slot MCA

The dimensions of the MCA are chosen so that it allows interstitial treatment of the cancer in a minimally invasive way.

Table 1: Dimensions of MCA

Materials	Dimensions (mm)
Inner conductor	0.37
Outer conductor	1.33
Dielectric	1.07
Catheter	1.65
Slot	2.00

Dimensions are summarized in Table 1. The slot position and width are calculated in order to achieve high localized power deposition near the distal tip of the antenna. The slot is positioned at about 5.5 mm from the short-circuited tip. This position gives lowest return loss at the operating frequency 2.45 GHz. It has been shown that the thickness of the catheter influences the power deposition and an increase in its thickness leads to a non localized SAR distribution [7].

2.2. Proposed single slot MCA

In order to suppress the backward heating effect along MCA and to obtain higher power deposition in front of the slot, we add to the outer conductor of the antenna an electrically connected T-ring shape structure.
The overall antenna is composed of the coaxial slot antenna around which the T-ring shape structure is wrapped. Figure 2 is a representation of the new antenna where we can see the added structure without the cathher.

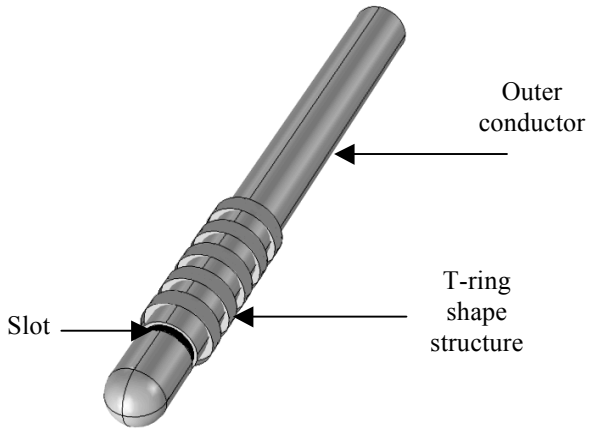

Figure 2: The new single slot MCA with T-ring shape structure wrapped around the outer conductor

Dimensions of the T-ring shape (Figure 3) are small compared to the effective wavelength in the liver, at the operating frequency. The wavelength is calculated according to the equation (1):

$$\lambda_{eff} = \frac{c}{f\sqrt{\varepsilon_r}} \qquad (1)$$

where c is the speed of light in free space [m/s], f is the operating frequency (2.45 GHz) and ε_r is the relative permittivity of the liver which is given in Table 2.

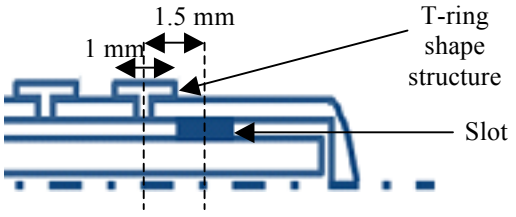

Figure 3: A 2D sectional view of the antenna with T-ring shape structure

If multiple T-ring shape structures are to be used, the spacing between them does not affect the overall behavior of our new antenna. However, in this study we consider a relatively small spacing compared to the effective wavelength. The spacing is equal to 1.5 mm.

2.3. Numerical modeling

The new MCA inserted in the liver tissue is modeled using finite elements method. The model uses a time-varying transverse electromagnetic (TEM) wave that is generated by the microwave source and propagating in the coaxial cable. The governing wave equation in the liver tissue, in term of the azimuthal magnetic field is:

$$\nabla \times ((\varepsilon_r - \frac{j\sigma}{\omega\varepsilon_0})^{-1} \nabla \times \vec{H}_\varphi) - \mu_r k_0^2 \vec{H}_\varphi = 0 \quad (2)$$

where ε_0, ε_r, μ_r, σ are respectively the permittivity of free space, the relative permittivity and permeability and the electrical conductivity of the liver tissue.
The dielectric properties of the liver that depend on the frequency are calculated using the Cole-Cole expression [12].

$$\varepsilon(\omega) = \varepsilon_\infty + \sum_{m=1}^{4} \frac{\Delta\varepsilon_m}{1 + (j\omega\tau_m)^{(1-\alpha_m)}} + \frac{\sigma_i}{j\omega\varepsilon_0} \quad (3)$$

Where, ε_∞ is the permittivity in the terahertz frequency range, σ_i is the ionic conductivity, τ is the relaxation time and $\Delta\varepsilon$ is the drop in the permittivity. Using the equation (3) that is explicitly written in term of its parameters that are tabulated in [13], the relative permittivity and the conductivity of the liver are respectively 43.03 and 1.686 S/m. These values together with antenna characteristics are given in Table 2.

Table 2: Materials properties

Material	Permittivity	Conductivity
Liver	43.03	1.686
Catheter	2.6	0
Dielectric	2.03	0
Air	1	0

The procedure for the analysis is as follows. First, the wave equation (2) is solved to find the electric field distribution in the liver. Next, the heat generated by the electric field in the tissue is calculated by the Specific Absorption Rate (SAR) that represents the time average of power deposited in the liver (W/kg). The SAR formula is given below.

$$SAR = \frac{\sigma|E|^2}{2\rho} \quad (4)$$

Where σ is electrical conductivity ρ is the tissue density and E is the electric field generated by the MCA.
Once the absorbed power is calculated, the thermal analysis is carried out by means of the Pennes' bioheat equation (5) that describes the transfer of heat in the liver tissue [14].

$$\rho C \frac{\partial T}{\partial t} = \nabla.(k_{th} \nabla T) + \rho_b C_b \omega_b (T_b - T) + Q_{met} + Q_{ext} \quad (5)$$

ρ_b is the blood density, C_b is the blood specific heat, k_{th} is tissue heat conductivity, ω_b is blood perfusion rate, T is tissue temperature and T_b is blood temperature and finally Q_{met} and Q_{ext} are respectively metabolic heat and the external heat generated by radiated microwave power. In tissue study the metabolic heat source Q_{met} is considered to be equal to zero and Q_{ext} is given by (6).

$$Q_{ext} = \frac{\sigma|E|^2}{2} = \rho.SAR \quad (6)$$

Thus, the bioheat equation (5) becomes:

$$\rho C \frac{\partial T}{\partial t} = \nabla.(k_{th} \nabla T) + \rho_b C_b \omega_b (T_b - T) + \rho.SAR \quad (7)$$

Parameters in equation (7) and their values are summarized in Table 3 [15].

Table 3: Tissue thermal characteristics

Parameters	Values
k_{th}	0.512 W/(m.K)
C_b	4800 J/(kg.K)
C	3600 J/(kg.K)
ρ_b	1000 kg/m^3
ρ	1060 kg/m^3
ω_b	3.6x10^{-3} 1/s
T_b	37 °C

The liver tissue is modeled in a cylindrical form and its material is considered to be uniform. In 2D the dimension of the tissue are 30 mm in large and 80 mm in depth. The MCA is inserted in the liver at an insertion depth of 70.5 mm.

The boundary conditions for the electromagnetic and thermal analysis are as follows: A TEM wave is excited at the inlet of the coaxial antenna. The wave is propagating in the coaxial antenna and it is radiated into the liver through the slot.

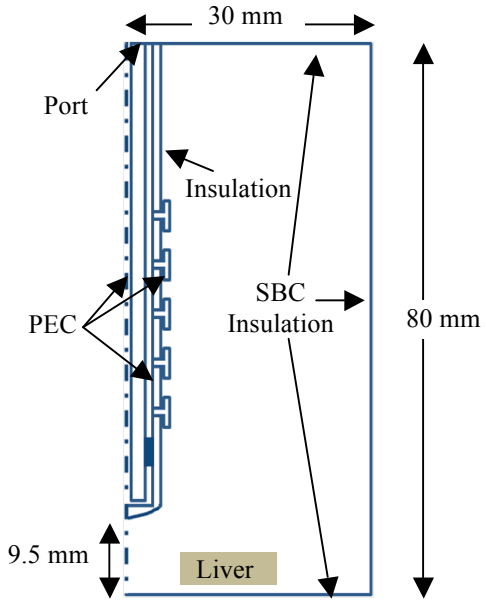

Figure 4: Model Geometry and Boundary Conditions

In order to prevent the outer sides of the liver to act as secondary sources, a scattering boundary condition (SBC) is applied. This boundary condition suppresses reflected waves from outer surfaces. The MCA conductors as well as the T-ring shape structures are considered to be perfect electric conductors (PEC).

Regarding to the thermal analysis, heat transfer is calculated only in the liver; therefore a thermal insulating boundary condition (TIBC) is applied on its boundaries. These conditions are summarized on Figure 4.

3. Results

In order to show the effectiveness of the new MCA, we plotted the SAR distribution along the antennas at 2.5 mm for the two types of MCA. In Figure 5 the black line represents the SAR for the classical MCA (without T-ring shape structure). The other curves are for the new antenna with the added structures where 1T, 3T,…, 9T correspond to the number of T-ring shapes. It is clearly shown that at the slot position (the slot is centered at 16.5 mm from the tip of the antenna), the SAR value is higher for the new MCA, whatever the number of the T-ring shape. The SAR is highest for the new MCA with 5 T-ring shape structures.

It is also demonstrated that, after 20 mm from the distal tip of the antenna, the SAR is considerably reduced compared to the classical single slot MCA. This effect is more significantly pronounced for the MCA with 1T-ring shape structure.

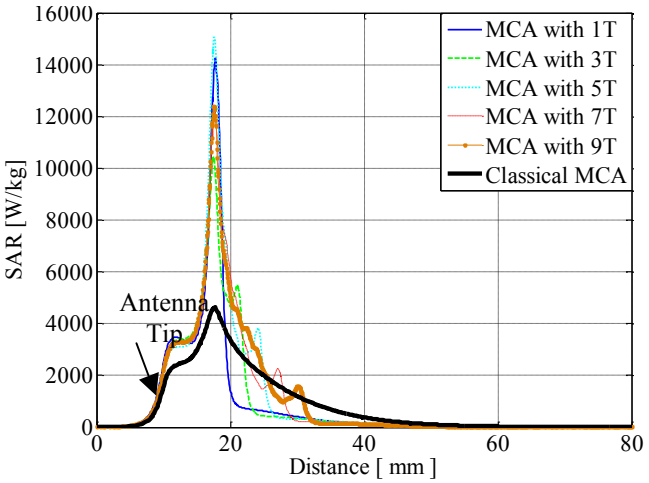

Figure 5: SAR distribution along the MCA at 2.5 mm

The effect of the T-ring shape structure on the antenna radiation pattern is more clearly apparent in 2D representation. The SAR distribution for both cases is qualitatively shown in Figure 6. One can observe that the radiated power is concentrated around the slot and the "tail" of the SAR pattern is lowered.

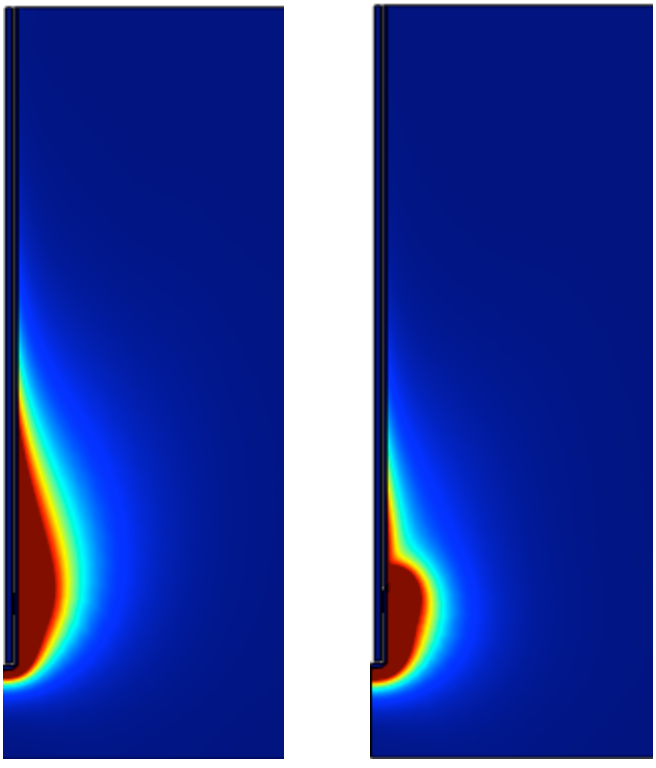

Figure 6: Microwave power absorbed in the liver for a) classical MCA b) new MCA with 1T-ring shape structure

Furthermore, as a consequence of the high localization of the absorbed power in the tissue, the rise in temperature is

higher for the new MCA. Once more, the temperature is higher for the new antenna with 5T-ring shape structure but the reduction of the backward heating effect is more significantly marked for the MCA with 1T-ring shape structure. Especially after 20 mm, the temperature along the MCA is lower with the new antenna (Figure 7).

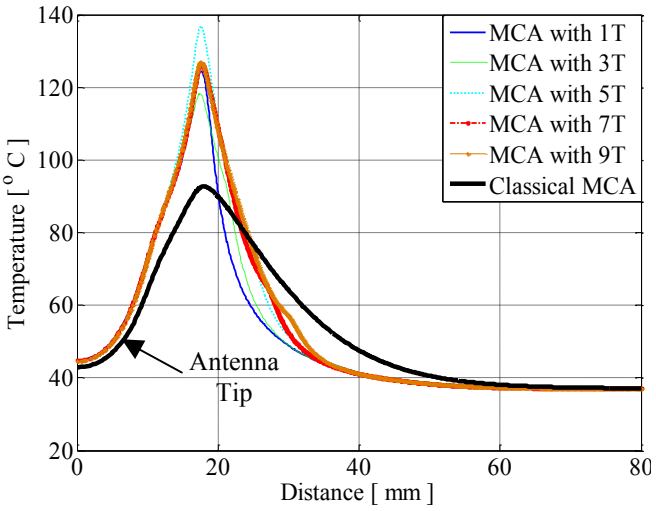

Figure 7: Temperature at 2.5 mm along MCA

We also performed a transient analysis of our MCA in the liver. The rise in tissue temperature (calculated at 2.55 mm in front of the slot) with respect to the heating time is given in Figure 8. First, one can notice that the temperature increases with increasing time for both antennas. Second, the rise in temperature is faster for our new design of MCA. After 240 s, the calculated temperature with the classical MCA is about 84 °C while it is between 106 °C and 119 °C when the T-ring shape structures are mounted on MCA. These results mean that one can reach the desired temperature within less time.

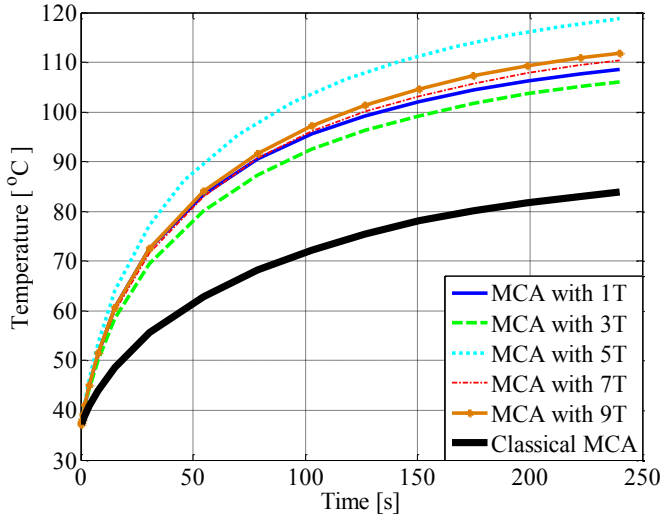

Figure 8: Temperature versus Time for both antennas

4. Conclusions

The new MCA with T-ring shape structure seems to achieve higher localized SAR distribution at the slot position than the classical one. The backward heating problem is also improved by the new antenna. Another improvement by the T-ring shape structure is obtained with shorter heating time which speeds the ablation operation up.

As a next step, these simulations results should be confirmed with experimental results on real liver tissue. Also, further improvements to the new model could be considered by changing the shape of the added structure.

References

[1] John Hopkins Pathology Liver Cancer website, http://pathology.jhu.edu/liver/index.cfm.

[2] The National Cancer Institute, NIH Publication No. 09-5009, http://www.cancer.gov/cancertopics/wyntk/liver

[3] S.B. Chinn, F.T. Lee, G.D. Kennedy,C. Chinn, C.D. Johnson, T.C. Winter, T.F. Warner, D.M. Mahvi, Effect of vascular occlusion on radiofrequency ablation of the liver: Results in a porcine model. Am J Roentgenol. 2001;176:789–95.

[4] R. Vilana, J. Bruix, C. Bru, C. Ayuso, M. Solé, J. Rodés, Tumor size determines the efficacy of percutaneous ethanol injection for the treatment of small hepatocellular carcinoma. Hepatology 1992;16(2): 353-7.

[5] A.S. Wright, D.M. Mahvi, D.G. Haemmerich, F.T. Lee, Minimally Invasive Approaches in Management of Hepatic Tumors, Surgical Technology International, 11:144-53, 2003

[6] P. Keangin, P. Rattanadecho, T. Wessapan, An analysis of heat transfer in liver tissue during microwave ablation using single slot antenna, International Communication in Heat and Mass Transfer, Vol. 38, 757-766, 2011.

[7] J. M. Bertram, D. Yang, M. C. Converse, J. G. Webster, and D. M. Mahvi, "A review of coaxial-based interstitial antennas for hepatic microwave ablation," *Crit. Rev. Biomed. Eng.*, Vol. 34, pp. 187213, 2006.

[8] P. Prakash, Theoretical Modeling for Hepatic Microwave Ablation, The Open Biomedical Engineering Journal, Vol. 4, 27-38, 2010.

[9] K. Saito, Y. Hayashi, H. Yoshimura, K. Ito, Heating characteristics of array applicator composed of two coaxial-slot antennas for microwave coagulation therapy, IEEE Transactions on Microwave Theory and Techniques 48, 1800–1806 (1 PART 1), 2000

[10] L. Hamada, Basic analysis on SAR distribution of coaxial-slot antenna array for interstitial microwave hyperthermia. IEICE Trans Electron, 78:1624–31, 1995.

[11] Y. Deshan, J.M. Bertram, M.C. Converse, A.P. O'Rourke, J.G. Webster, S.C. Hagness, J.A. Will, D.M. Mahvi, "A floating Sleeve Antenna Yields Localized Hepatic Microwave Ablation", IEEE Transaction on Biomedical Engineering, Vol. 53, No. 3, March 2006.

[12] C. Gabriel, Compilation of the Dielectric Properties of Body Tissues at RF and Microwave Frequencies. King's College London (United Kingdom) Dept. Of Physics, 1996.
[13] S. Gabriel, R. W. Lau, and C. Gabriel, "The dielectric properties of biological tissues: III. parametric models for the dielectric spectrum of tissues," *Phys. Med. Biol.*, vol. 41, pp. 2271–2293, 1996.
[14] H.H. Pennes, Analysis of tissue and arterial blood temperatures in the resting human forearm, Journal of Applied Physiology 85 (1), 5–34, 1998.
[15] T. Jiao, H. Wang, Y. Zhang, X. Yu, H. Xue, H. Lv, X. Jing, H. Zhan, J. Wang, A coaxial-slot antenna for invasive microwave hyperthermia therapy, J. Biomedical Science and Engineering, 5, 202-206, 2012.